Active Site Mutations and Substrate Inhibition in Human Sulfotransferase 1A1 and 1A3

THE JOURNAL OF BIOLOGICAL CHEMISTRY
Vol. 279, No. 18, Issue of April 30, pp. 18799–18805, 2004

Printed in U.S.A.

Active Site Mutations and Substrate Inhibition in Human Sulfotransferase 1A1 and 1A3*

Received for publication, November 10, 2003, and in revised form, January 28, 2004
Published, JBC Papers in Press, February 10, 2004, DOI 10.1074/jbc.M312253200

Amanda C. Barnett‡, Sergey Tsvetanov‡, Niranjali Gamage‡, Jennifer L. Martin§¶, Ronald G. Duggleby‖, and Michael E. McManus‡**

From the ‡School of Biomedical Sciences, §Institute for Molecular Bioscience, and ‖School of Molecular and Microbial Sciences, University of Queensland, Brisbane, Queensland 4072, Australia

Human SULT1A1 is primarily responsible for sulfonation of xenobiotics, including the activation of promutagens, and it has been implicated in several forms of cancer. Human SULT1A3 has been shown to be the major sulfotransferase that sulfonates dopamine. These two enzymes shares 93% amino acid sequence identity and have distinct but overlapping substrate preferences. The resolution of the crystal structures of these two enzymes has enabled us to elucidate the mechanisms controlling their substrate preferences and inhibition. The presence of two *p*-nitrophenol (*p*NP) molecules in the crystal structure of SULT1A1 was postulated to explain cooperativity at low and inhibition at high substrate concentrations, respectively. In SULT1A1, substrate inhibition occurs with *p*NP as the substrate but not with dopamine. For SULT1A3, substrate inhibition is found for dopamine but not with *p*NP. We investigated how substrate inhibition occurs in these two enzymes using molecular modeling, site-directed mutagenesis, and kinetic analysis. The results show that residue Phe-247 of SULT1A1, which interacts with both *p*-nitrophenol molecules in the active site, is important for substrate inhibition. Mutation of phenylalanine to leucine at this position in SULT1A1 results in substrate inhibition by dopamine. We also propose, based on modeling and kinetic studies, that substrate inhibition by dopamine in SULT1A3 is caused by binding of two dopamine molecules in the active site.

The cytosolic sulfotransferase (SULT)[1] gene superfamily encodes enzymes catalyzing sulfonation of numerous xeno- and endobiotics, such as drugs, hormones (*e.g.* 17β-estradiol, thyroid hormones, and dehydroepiandrosterone), chemical carcinogens, bile acids, and neurotransmitters. These substrates may undergo sulfonation directly as in phase II metabolism (*e.g.* minoxidil, paracetamol) or following phase I metabolism after introduction of a functional hydroxyl group (*e.g. N*-hydroxyl arylamines). The sulfonate donor for these reactions is 3′-phosphoadenosine 5′-phosphosulfate (PAPS; Refs. 1–3). Sulfonation is generally considered to be a detoxification pathway for a broad range of compounds, because conjugation with a sulfonate (SO_3^{-1}) renders substrates more hydrophilic and facilitates their excretion. However, evidence has emerged in recent years that this reaction can lead to formation of highly reactive intermediates (*e.g.* with N-hydroxy heterocyclic and aromatic arylamines) that can bind to DNA resulting in mutagenicity and carcinogenicity (4–6). Therefore, various studies have investigated its role in human cancer and in particular polymorphisms in SULT1A1 have been implicated in the predisposition to lung cancer (7), age of onset in breast cancer (8), and increased risk of breast cancer (9, 10).

Fifty-six cytosolic SULT cDNAs have been cloned and characterized from bacteria to human (11–13). SULT1, SULT2, SULT3, SULT4, and SULT5 gene families have been identified in mammals. Of these, only SULT1, SULT2, and SULT4 have been identified in humans. These include seven members of the SULT1 family (SULT1A1, SULT1A2, SULT1A3, SULT1B1, SULT1C1, SULT1C2, and SULT1E1), two members of the SULT2 family (SULT2A1 and SULT2B), and one member of the SULT4 family (SULT4A1). Although each SULT has distinct substrate preferences, the range of molecules accepted can be broad and may be overlapping. In general, the SULT1 family catalyzes sulfonation of small phenols, monoamine neurotransmitters (*e.g.* dopamine), thyroid hormones, and estrogens, and the SULT2 family sulfonates steroid hormones. To date, neither an endogenous nor an exogenous substrate has been found for SULT4 A1.

Although there has been an increase in structure function studies as a result of an expansion of SULT x-ray crystal structures published, substrate binding and inhibition mechanisms are still far from clear. The crystal structures of mouse estrogen SULT1E1 (14), human SULT1A3 (15, 16), SULT domain of the human membrane bound heparan sulfate *N*-deacetylase/*N*-sulfotransferase 1 (17), human hydroxysteroid SULT2A1 (18, 19), and human estrogen SULT1E1 (20); in addition, site-directed mutagenesis of critical amino acids in these enzymes has provided information on catalytic mechanism of these enzymes. Recently, this laboratory also reported the structure of human SULT1A1, crystallized in the presence of 3′-phosphoadenosine 5′-phosphate (PAP) with two *p*-nitrophenol (*p*NP) molecules bound in the active site (21). This structure is similar to the other SULT enzymes as it incorporates a core PAP binding site. However, it was the first structure to show two molecules of the substrate bound in the active site.

Substrate inhibition is characteristic of many SULT enzymes and has been reported previously with human SULTA1 and SULT1A3 with *p*NP and dopamine, respectively (22–24). The presence of two substrate molecules in the SULT1A1 structure was postulated to explain the slight cooperativity observed

* This work was supported by National Health and Medical Research Council of Australia Grant 252734. The costs of publication of this article were defrayed in part by the payment of page charges. This article must therefore be hereby marked "*advertisement*" in accordance with 18 U.S.C. Section 1734 solely to indicate this fact.

¶ Supported by a fellowship from the Australian Research Council.

** To whom correspondence should be addressed: Faculty of Biological and Chemical Sciences, Computer Science Building (Bldg. 69, Rm. 304), University of Queensland, Queensland 4072, Australia. Tel.: 61-7-3365-1609; Fax: 61-7-3365-1613; E-mail: m.mcmanus@uq.edu.au.

[1] The abbreviations used are: SULT, sulfotransferase; PAPS, 3′-phosphoadenosine 5′-phosphosulfate; *p*NP, *p*-nitrophenol.

at low concentrations of substrate and the inhibition observed at higher concentrations of pNP. In previous work (21), we proposed that inhibition is caused by impeded catalysis when both binding sites are occupied. In SULT1A1, substrate inhibition is evident when the *p*NP is used as the acceptor molecule but not when dopamine is the substrate. To investigate this further, we modeled dopamine into the substrate-binding pocket of SULT1A1 to show that two dopamine molecules could fit. Dopamine is the preferred substrate of SULT1A3 and our initial resolution of SULT1A3 structure showed large stretches of disorder that account for about 25% of its structure, which may in part be caused by lack of substrate binding (15). Therefore, we have also modeled the substrate-binding pocket of SULT1A3 to investigate dopamine binding and to determine how substrate inhibition takes place in this enzyme. Finally, site-directed mutagenesis was performed on residues interacting with the substrate molecule at the active site of SULT1A1 indicated that the flexible residue Phe-247 is important for substrate inhibition by dopamine.

MATERIALS AND METHODS

SULT1A1 and SULT1A3 were previously subcloned into the pET 28a(+) vector (Novagen, Victoria, Australia). The substrates dopamine, *p*NP, and PAPS were purchased from Sigma. [^{35}S]PAPS was purchased from Amrad Pharmacia Biotechnology (Victoria, Australia). The primers for sequencing and site-directed mutagenesis were obtained from PROLIGO (New South Wales, Australia). The PCR kit *Pfu*-Turbo was obtained from Stratagene. The restriction enzyme DpnI was purchased from New England Biolabs. All other reagents were of molecular biology or analytical grade.

Site-Directed Mutagenesis—Double-stranded primers encoding a single amino acid mutation in the SULT1A1 gene were used to obtain SULT1A1 mutants. Twenty cycles of PCR were carried out with denaturation at 94 °C for 30 s, annealing at 55 °C for 1 min, and extension at 68 °C for 12 min. The reaction contained 50 ng of DNA template, primers, 200 μM concentrations of each of the four deoxynucleotide triphosphates (dNTPs), 1× *Pfu*Turbo buffer, and 2.5 units of *Pfu*Turbo DNA polymerase. The PCR product was treated with DpnI for 1 h at 37 °C followed by transformation of BL21 (DE3) *Escherichia coli* cells. The transformed bacteria were used to amplify the plasmid for sequencing as well as for protein expression of the SULT1A1 mutants. The mutated cDNA sequences were confirmed by automated sequencing carried out by the Australian Genome Research Facility (Brisbane, Australia) with the ABI Prism dye terminator cycle sequencing ready reactions (PerkinElmer Life Sciences) using the T_7-promoter and terminator universal primers.

Expression, Purification, and Enzyme Activity—Expression of the recombinant proteins was performed as described previously (15, 25, 26). The protein was purified utilizing the hexahistadine tag on the N terminus of the SULT1A1 and SULT1A3 cDNAs by TALON cobalt affinity (Clontech Laboratories) chromatography. Protein purity was estimated by SDS-polyacrylamide gel electrophoresis and only fractions with the highest purity were used for enzyme assay. The purified protein was mixed with glycerol to a final concentration of 20% (v/v) and stored at −70 °C before use. Protein concentration was determined by the BCA method (Sigma).

Enzyme activity assays were performed using the method described by Foldes and Meek (27) as modified by Brix *et al.* (26). The reaction mixture consisted of 20 μM [^{35}S]PAPS, 0.1 μg/ml SULT1A1, 10 mM potassium phosphate buffer, pH 7.0, and varying concentrations of the substrates in a final volume of 500 μl. Reactions were started by adding the enzyme to the reaction mixture and then incubated for 20 min at 37 °C. The reaction was terminated by adding 0.1 M barium hydroxide, 0.1 M barium acetate, and 0.1 M zinc sulfate, precipitating the enzyme and unreacted [^{35}S]PAPS. Assays were performed in duplicate and the radioactivity of the sulfonated product was determined using a liquid scintillation counter (Tri-Carb 2500; PerkinElmer Life and Analytical Sciences). The incubation time and protein concentration used were chosen to be within the linear range for product formation.

Kinetic Data Analysis—Kinetic experiments were analyzed by nonlinear regression, fitting the appropriate equation to the data. This regression analysis was performed using the Grafit program, version 5 (Erithacus Software Limited, Surrey, UK).

Molecular Modeling—Modeling of substrates into the human SULT1A1/SULT1A3 substrate-binding pocket was performed using the docking program GOLD (Cambridge University) with 10 genetic algorithm runs and default parameters (28). The structure of SULT1A3 was modeled using the crystal structure of human SULT1A1 (Protein Data Bank code 1LS6) and minimized in Crystallography and NMR System software (29). The quality of the model was assessed with Procheck (30).

RESULTS

Molecular Modeling—Previously we proposed a kinetic model for SULT1A1 that explains slight cooperativity at very low substrate concentrations and inhibition at high substrate concentrations of *p*NP (21). When *p*NP is utilized as the acceptor molecule for SULT1A1, substrate inhibition is observed above 2 μM (Fig. 1*a*). However, when dopamine is used as the acceptor molecule, no obvious substrate inhibition is seen (Fig. 1*b*). The reverse is found for SULT1A3 (Fig. 1, *c* and *d*), where the preferred substrate dopamine exhibits substrate inhibition above 9 μM, whereas *p*NP follows Michaelis-Menten kinetics. The analysis of the crystal structure of SULT1A1 shows that two *p*NP molecules can be accommodated in the substrate-binding pocket (Fig. 2*a*). To investigate why there is no substrate inhibition of SULT1A1 by dopamine, we modeled this substrate into the active site of SULT1A1 (Fig. 2*b*).

Our model of SULT1A1 with dopamine showed that the substrate-binding pocket could accommodate two molecules of dopamine, although some "clashes" were observed with a residue that seemed to have some flexibility (Phe-247) when positioning the second dopamine molecule. With a small shift in orientation, either the 3-OH or 4-OH of dopamine could be oriented for sulfonation. Because 3-*O* sulfonated dopamine is reported to be high in humans (16), the dopamine was orientated for sulfonation at the 3-O position. In this orientation, it seems to form close contacts with the flexible Phe-247 and Val-148. By rotating Phe-247 to an alternate conformation (Fig. 2*b*), the two dopamine molecules could fit within the substrate-binding pocket. To determine whether the smaller leucine residue, found at this position in human SULT1A3, facilitates the binding of second dopamine molecule, we modeled the substrate-binding pocket of SULT1A3 using the SULT1A1 structure and investigated the positioning of two dopamine molecules in the substrate-binding pocket.

A computer model of SULT1A3 was constructed using the coordinates of SULT1A1 obtained from the Protein Data Bank (code 1LS6). Both enzymes have 295 residues, and 21 residues differ between these two enzymes. In the SULT1A1 structure, these residues were mutated to the corresponding SULT1A3 residues, the model was energy minimized in Crystallography and NMR System software, and the validity of the model was assessed. The backbone residues in the SULT1A3 model can be superimposed on the SULT1A1 crystal structure (295 Cα atoms with root-mean-square deviation 1.6 Å). PAPS was modeled into SULT1A3 based on the SULT1E1-PAPS structure (Protein Data Bank code 1HY3; Ref. 20) and dopamine was docked using the GOLD program with default parameters. The model of SULT1A3 (Fig. 2*c*) with dopamine showed that two molecules of substrate are easily accommodated in the substrate-binding pocket; positioning of the second dopamine molecule was easier with a leucine residue at position 247.

Kinetic Analysis—Previously, we analyzed the substrate saturation and substrate inhibition kinetics of SULT1A1 toward *p*NP using an equation (Equation 1) derived from the observation that the enzyme structure contains two bound substrate molecules (21).

$$v = V_\infty[S](K_1 + [S])/(K_2K_3 + [S]K_3 + [S]^2) \quad \text{(Eq. 1)}$$

The difficulty with this equation is that it contains three kinetic constants (K_1, K_2, and K_3) that have no obvious physical meaning. Only V_∞, the rate as [S] → ∞, relates directly to an

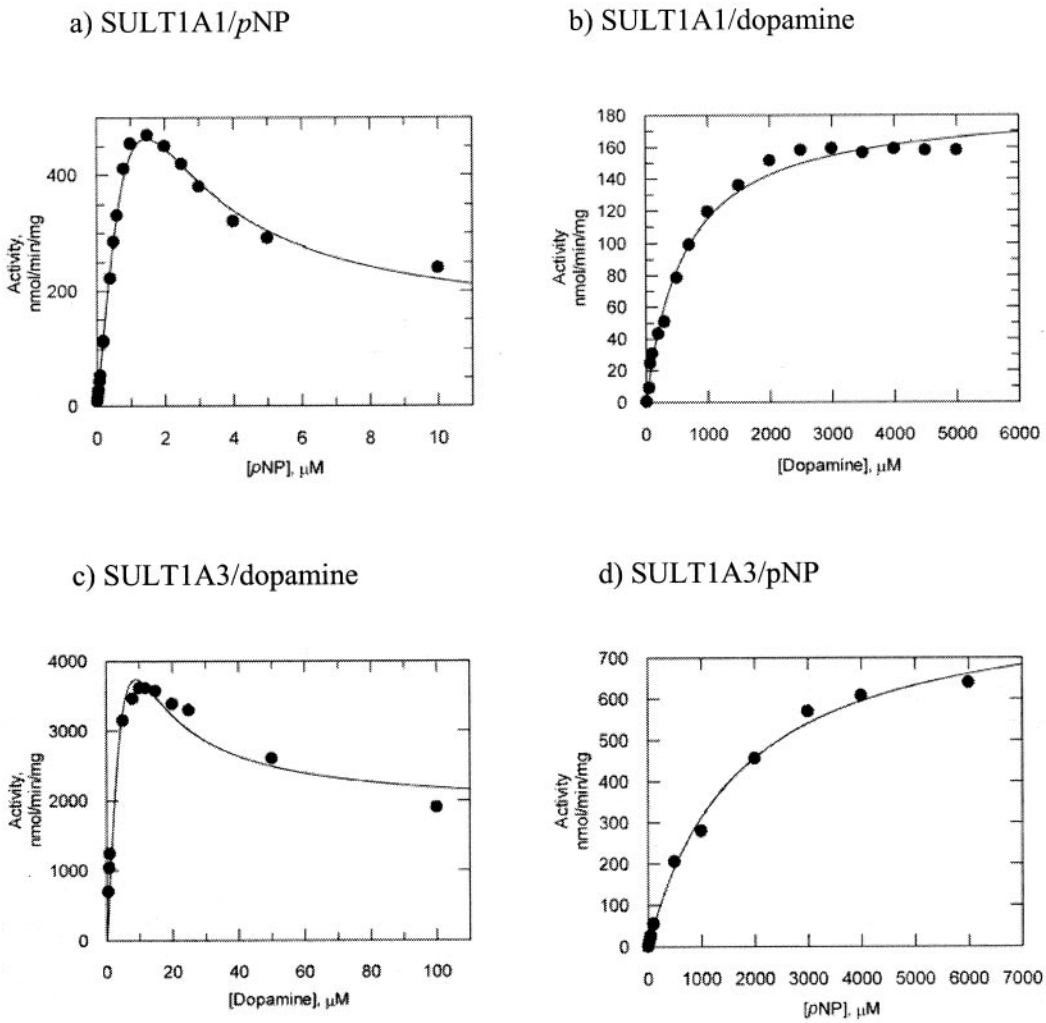

FIG. 1. **Kinetics of wild-type SULT1A1 and SULT1A3 toward *p*NP and dopamine.** Each data point (●) is an average of duplicate assays, and the standard deviation is contained within the dimensions of the circle. *a*, activity of SULT1A1 with *p*NP as the substrate with the concentrations up to 10 μM. *b*, SULT1A1 with dopamine concentrations up to 5 mM. *c*, activity of SULT1A3 with dopamine as the substrate with concentrations up to 100 μM. *d*, *p*NP concentrations up to 6 mM. In *a* and *c*, the line represents the best fit to the data of Equation 3, whereas in *b* and *d*, the line represents the best fit to the data of Equation 6.

observable quantity. We realized that this equation may be rewritten in terms of more normal constants,

$$v = (V_m[S] + V_\infty[S]^2/K_i)/(K_m + [S] + [S]^2/K_i) \quad \text{(Eq. 2)}$$

where V_m and K_m are the conventional maximum velocity and Michaelis constant, respectively, that would be observed if there were no substrate inhibition, whereas K_i is the substrate concentration that would give a rate midway between V_m and V_∞, if K_m was very small. Although this equation fits the data very well, the nonlinear regression analysis showed that there are extremely high parameter correlations between the pairs V_m and K_m, V_m and K_i, and K_m and K_i. This means that estimates of each of the parameters are unreliable because the values are highly dependent upon one another.

Further investigation showed that an empirical simplification could eliminate one parameter and these undesirable correlations, while maintaining a good fit. The revised equation is as follows.

$$v = (k_s[S] + V_\infty[S]^2/K_s^2)/(1 + [S]^2/K_s^2) \quad \text{(Eq. 3)}$$

The parameter k_s is the specificity constant, which corresponds to the ratio V_m/K_m for an enzyme that exhibits Michaelis-Menten kinetics. Graphically, it is the slope of the tangent to the activity *versus* [substrate] curve at the origin. The specificity constant can be used to directly compare the efficiencies of different enzymes (or mutants) for any given substrate, or different substrates with any given enzyme. V_∞ has the same definition as in Equations 1 and 2. The third parameter, K_s, is a "substrate constant" with no exact physical meaning but that acts as a scaling factor for the substrate concentration axis. It can be used as an intermediate vehicle to calculate the more meaningful parameters S_p (the concentration of substrate that results in the peak rate) or V_p (the rate at $[S] = S_p$) using the relationships below.

$$S_p = (K_s^2 + 2V_\infty/k_s)^{1/2} \quad \text{(Eq. 4)}$$

$$V_p = k_s S_p/2 \quad \text{(Eq. 5)}$$

Although it would be desirable to use Equation 2 for the data analysis, we believe that it is preferable to use an Equation that yields reliable parameter values even though it has an empirical element. Kinetic data that exhibit substrate inhibition were fitted using the combined Equations 3, 4, and 5 to obtain best fit values and standard errors for k_s, V_p, and V_∞. Where data showed no substrate inhibition, a reparameterized version of the Michaelis-Menten Equation 6 was used for the analysis to obtain best fit values and standard errors for k_s and V_m.

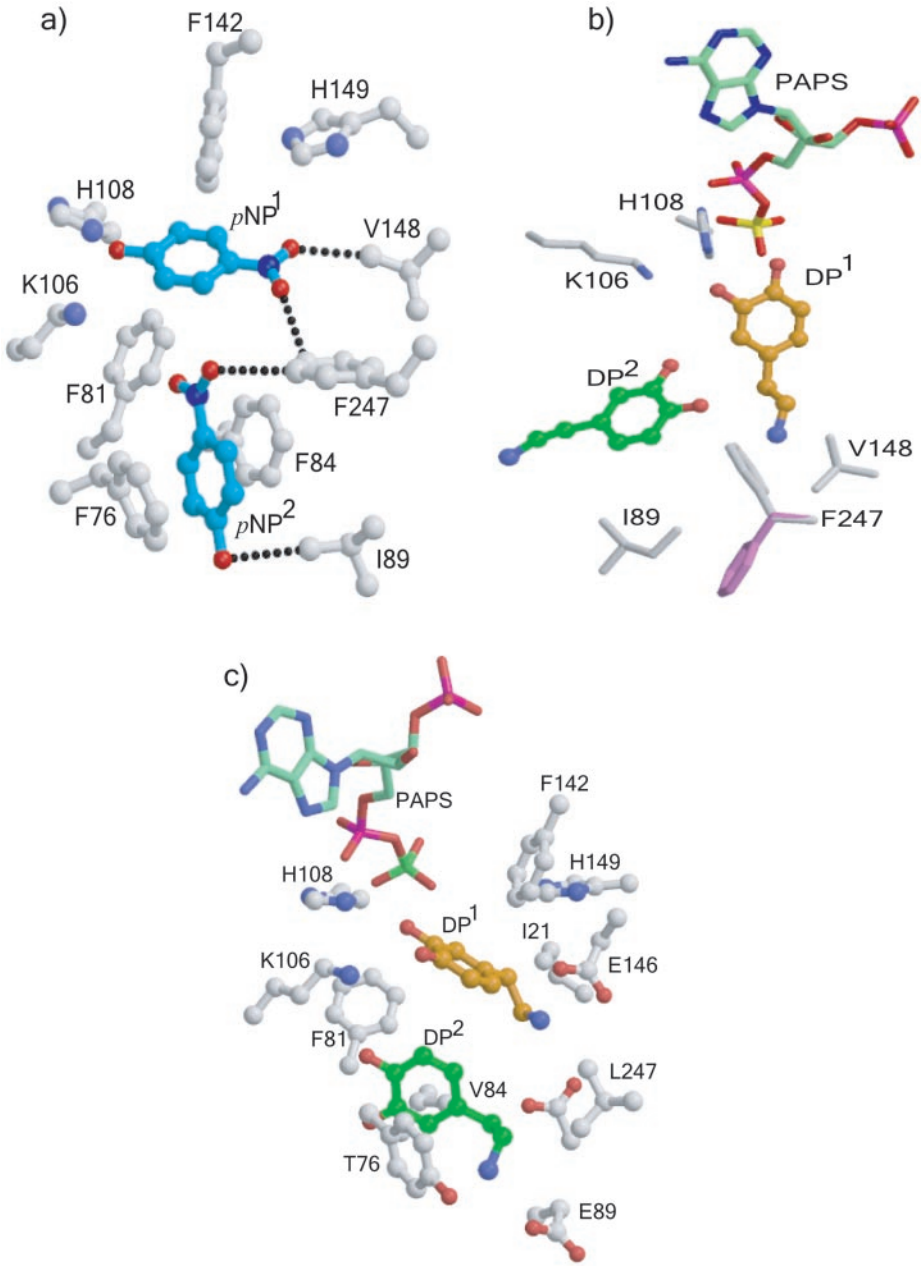

FIG. 2. *a*, *p*NP interactions with the SULT1A1 binding pocket as shown by the crystal structure of SULT1A1. *p*NP[1] shows van der Waals interactions (shown by *dotted lines*) with Val-148 and Phe-247 and *p*NP[2] shows interactions with Phe-247 and Ile-89. The residues that are present in the substrate binding pocket but not shown for clarity are Ile-21, Phe-24, Met-77, Pro-90, Ala-146, Tyr-169, Tyr-240, and Val-243. *b*, SULT1A1 structure with dopamine modeled into the substrate-binding pocket. The alternate conformation of residue Phe-247, which allows the binding of second dopamine molecule (*DP*[2]), is shown in *pink*. The residues not shown for clarity are Ile-21, Phe-24, Met-77, Pro-90, Ala-146, Tyr-169, Tyr-240, and Val-243. *c*, substrate-binding pocket of the modeled SULT1A3 structure. The binding mode of two dopamine molecules and PAPS is shown. Residues not shown for clarity are Ile-21, Phe-24, Pro-90, Tyr-240, Val-243, and Met-248. The catalytically active dopamine molecule 1 (*DP*[1]) is shown in *orange* and dopamine 2 (*DP*[2]) in *green*. PAPS is shown as a stick model.

$$v = k_s[S]/(1 + k_s[S]/V_m) \quad \text{(Eq. 6)}$$

To determine whether substrate inhibition involves the three residues that interact with both *p*NP molecules (Ile-89, Phe-247, and Val-148; Fig. 2*a*), in particular residue 247 as suggested by the computer modeling, we employed site-directed mutagenesis. Residues 247 and 148 were exchanged to their counterpart residues in human SULT1A3 (F247L, V148A), whereas residue 89 was converted to the smaller alanine residue. His-108 was not mutated because it is reported to function as a catalytic residue for sulfonation (31, 32) and is found in all human sulfotransferases.

SULT1A1-F247L—When modeled into the SULT1A1 structure, the leucine in the mutant of phenylalanine at 247 to leucine (F247L) does not form van der Waals interactions with the nitro groups of *p*NP[1] and *p*NP[2], but there is no change to the overall protein structure. Unlike wild-type human SULT1A1 with dopamine, this mutant showed substrate inhibition when dopamine was used as the acceptor molecule (Fig. 3*a*) and retained substrate inhibition with *p*NP (Fig. 3*b*). When this mutant was analyzed kinetically, it showed an increased affinity for *p*NP (Table I) and exhibited substrate inhibition at a slightly lower *p*NP concentration.

Using Equation 3, we find that in the F247L mutant, there is an increase of approximately 2-fold in the specificity constant (k_s) for both substrates, although neither the peak rate (Equation 5) nor the limiting rate for SULT1A1-F247L is significantly different when *p*NP is the acceptor molecule (Table I). With dopamine as substrate, the peak rate is similar to V_m when compared with the wild-type enzyme, with substrate inhibition exhibiting a limiting rate of 78.9 nmol/min/mg (Table I).

SULT1A1-V148A and SULT1A1-I89A—In the SULT1A1 crystal structure, the mutation of valine at 148 to alanine (V148A) removes van der Waals interaction to the nitro group of *p*NP[1]. The mutation of isoleucine at 89 to alanine (I89A) disrupts the binding of *p*NP[2] to the enzyme. These mutants did not show any significant effect on substrate inhibition pattern with dopamine or *p*NP (Table I).

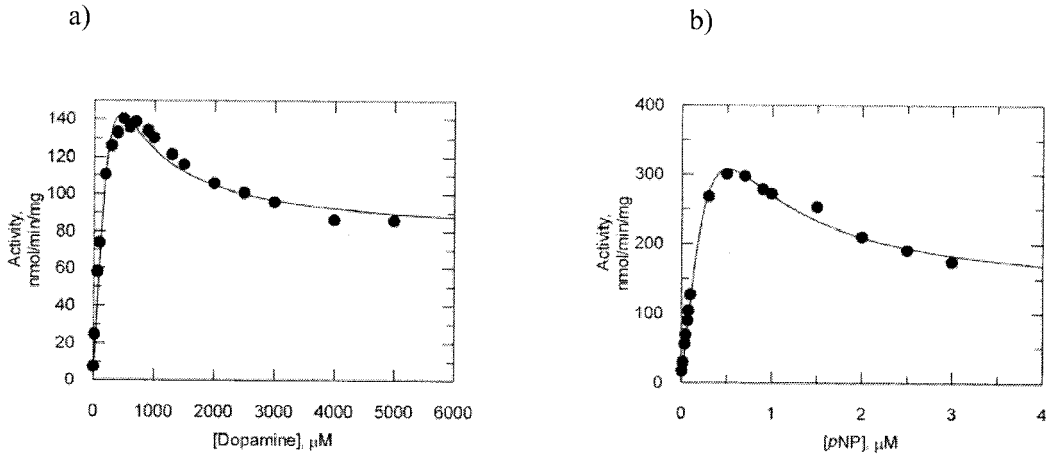

FIG. 3. **Kinetics of the SULT1A1-F247L mutant toward *p*-nitrophenol and dopamine.** Each data point (●) is an average of duplicate assays, and the standard deviation is contained within the dimensions of the circle. *a*, activity of F247L mutant as a function of dopamine concentration up to 5 mM; *b*, *p*NP to 3 μM. The *lines* represent the best fit to the data of Equation 3.

TABLE I
Kinetics of SULT1A1 wild type and the F247L, V148A, and I89A mutants

The specificity constant (k_s) is equivalent to V_m/K_m in Michaelis-Menten kinetics, where V_m is the maximum velocity and K_m is the Michaelis constant. For cases in which substrate inhibition is observed, V_p is the rate at the peak, whereas rate V_∞ is the limiting rate [S] → ∞.

Enzyme	Substrate	k_s	V_m	V_p	V_∞
		ml/min/mg	*nmol/min/mg*	*nmol/min/mg*	*nmol/min/mg*
Wild type	*p*NP	636 ± 14	N.A.[a]	464 ± 6	125 ± 16
F247L	*p*NP	1211 ± 37	N.A.	308 ± 4	123 ± 9
V148A	*p*NP	2210 ± 52	N.A.	491 ± 5	117 ± 9
I89A	*p*NP	2672 ± 90	N.A.	746 ± 11	158 ± 16
Wild type	Dopamine	0.302 ± 0.021	187 ± 4	N.A.	N.A.
F247L	Dopamine	0.638 ± 0.033	N.A.	142 ± 3	79 ± 5
V148A	Dopamine	0.425 ± 0.023	64 ± 0.9	N.A.	N.A.
I89A	Dopamine	1.154 ± 0.128	219 ± 6	N.A.	N.A.

[a] N.A., not applicable.

DISCUSSION

Substrate inhibition is a characteristic feature of many sulfotransferases, observed usually at high concentrations of their preferred substrates. However, in general, the Michaelis-Menten model has been used to explain catalysis by SULT1A1 and SULT1A3 at moderate substrate concentrations (26, 33). In previous work, we proposed a model that links the observed substrate inhibition to the finding that there are two substrate molecules bound near to the active site in the crystal structure of SULT1A1 (21). One substrate molecule (pNP^1) is in the correct position for sulfonation, whereas the other (pNP^2) blocks the channel that leads to the active site. In this model, inhibition results because the rate constant for catalysis is higher when pNP^2 is absent than when it is present. Thus, there is impeded catalysis when both binding sites are occupied, which we imagine is caused by molecular crowding that perturbs the positioning of pNP^1. In addition, when the pNP^2 alone is bound, access to the active site is prevented. The combination of these two effects results in the observed substrate inhibition.

In our present study, the differing patterns of substrate inhibition relating to the substrates (*p*NP and dopamine) of SULT1A1 and SULT1A3 suggested to us that the substrate-binding pocket of SULT1A1 may not accommodate two molecules of dopamine or that binding of the second substrate molecule may have been impeded in some way. To investigate this, we modeled dopamine into the substrate-binding pocket of the human SULT1A1 structure. We found that the substrate-binding pocket of SULT1A1 could accommodate two molecules of dopamine, although one enzyme residue (Phe-247) made unfavorable interactions with the second molecule. This led us to hypothesize that this residue may be important in substrate inhibition. Site-directed mutagenesis of Phe-247 to the smaller leucine residue found in SULT1A3 gave rise to substrate inhibition in SULT1A1, suggesting that dopamine can be accommodated in the second binding site without making unfavorable interactions with the enzyme. Therefore, this residue seems to be involved in the phenomenon of substrate inhibition, because mutations in other residues that interact with *p*NP (Ile-89 and Val-148) exhibited kinetic profiles that are similar to the wild-type SULT1A1.

The size and nature of the substrate binding pocket of SULT1A1 and SULT1A3 suggest that much larger molecules than *p*NP can be accommodated. Endogenous substrates such as iodothyronines and 17β-estradiol (E2) have shown to be catalyzed by SULT1A1 with a clear substrate inhibition (34, 35). SULT1A3 also sulfonates the above substrates with a low affinity (34, 36), and higher concentrations of these substrates needed to be analyzed to investigate substrate inhibition. In fact, 3,3′-diiodothyronine (T2) was recently identified as the endogenous substrate of SULT1A1 (37), and we identified a catalytically feasible binding conformation when T2 modeled into the active site of SULT1A1 (21). In this conformation, the two phenyl rings of T2 occupy each of the *p*NP binding sites by adopting a bent conformation. We also discussed in the same article that a rigid multi-ring substrates such as E2 cannot accommodate the binding pocket without a conformational change in the enzyme. However, with both T2 and E2, it is unlikely that two molecules will occupy the substrate binding site of these two isozymes. Therefore, substrate inhibition would probably occur by some other mechanism.

It is important to note that in the case of SULT1A1, Chen *et*

al. (38) have reported that residues Glu-83, Asp-134, Glu-246, and Asp-263 are involved in the catalytic activity of SULT1A1 based on their SULT1A1 model. However, the crystal structure of SULT1A1 suggests that the impaired activity seen with mutations of these residues is caused by a perturbation of the β4 strand and α6 helix, potentially disrupting the structure of the backbone. In a recent publication, the same authors (39) used their SULT1A1 model (although the crystal structure of SULT1A1 was published at the time) to demonstrate the importance of arginine residues for SULT1A1 catalytic activity. For example, they showed that when arginine at position 78 was mutated to a glutamic acid (R78E), SULT1A1 lost its activity for 2-naphthol, whereas when it was mutated to alanine (R78A), the enzyme retained activity. Based on their SULT1A1 model, they suggested that the positive charge at position 78 is not critical for activity. When it was mutated to a negatively charged residue, there was a significant reduction in activity, which they suggested was caused by an effect on lysine 106 (Lys-106). However, the SULT1A1 crystal structure shows that Lys-106 is 12 Å from Arg-78 and therefore unlikely to be affected by the mutation. A more likely cause is a disruption of a hydrogen bond or charge-charge interaction network involving Asp-59 and Gln-56. These two residues are located on the α2 helix just preceding the phosphate sulfate binding loop, which is critical for PAPS binding (14, 16, 20, 21). The crystal structure suggests that the R78E mutant would probably disrupt this network, thereby destabilizing PAPS binding because of unfavorable charge-charge interactions.

The crystal structure of the major catecholamine sulfotransferase, SULT1A3, was the first three-dimensional structure of a human cytosolic sulfotransferase to be solved. This structure was published simultaneously by both our group (15) and Coughtrie and co-workers (16). The Bidwell *et al.* (15) structure was solved with a sulfate ion bound at the active site, whereas the Dajani *et al.* (16) structure was complexed with the product 3′-phosphoadenosine 5′-phosphate. Significantly, both groups reported that about 25% of the SULT1A3 structure consisted of disordered regions, probably because of the lack of a bound substrate. Most of the 68 disordered residues in the apoSULT1A3 structure correspond to the substrate-binding regions in SULT1A1 (21).

When examining the model of SULT1A3, it highlighted the importance of residue 247 (leucine in SULT1A3 and phenylalanine in SULT1A1) in accommodating two dopamine molecules in the substrate binding site. These modeling data convincingly demonstrate that the observed substrate inhibition in SULT1A3 with dopamine is caused by impeded catalysis when two molecules of dopamine are present in the active site. The molecular mechanism of this substrate inhibition can be explained by using the proposed kinetic model for SULT1A1 (21).

In contrast to SULT1A1, the modeled SULT1A3 substrate-binding pocket has more charged residues, such as aspartate and glutamate (Fig. 2*c*), and these would favor binding of substrates having positively charged groups, such as dopamine. The model not only highlighted the importance of residue 247 but also showed the importance of three other residues: Asp-86, Glu-89 and Glu-146 for substrate interaction. With the aid of molecular modeling (based on the mouse SULT1E1 structure) and site-directed mutagenesis, we and others have previously identified these three residues as responsible for the high dopamine affinity of SULT1A3 (26, 40–42). In our SULT1A3 model, Glu-146 is placed within hydrogen-bonding distance of the amino group of the first dopamine molecule (Fig. 2*c*). The importance of this interaction in dopamine sulfonation is confirmed by the functional studies of Brix *et al.* (41). They have shown that by changing Glu-146 in SULT1A3 to glutamine (abolishing the negative charge), there is a 360-fold decrease in the specificity constant for dopamine. Furthermore, the change of a single amino acid, E146A, in SULT1A3 was sufficient to change the catalytic properties and substrate specificity so that it mimicked those of SULT1A1 (40, 41, 43). A related study from our laboratory showed that the mutant A146E in SULT1A1 yielded a SULT1A3-like protein with respect to *p*NP (41). Taken together, these data provide strong evidence that residue 146 is crucial for recognition of dopamine and determining the substrate specificity in SULT1A1 and SULT1A3.

Mn^{2+} has shown to stimulate dopamine sulfonation by SULT1A3, and this is proposed to occur via interaction between Mn^{2+} and Asp-86 which is in the mobile loop having residues 86–90 (44, 45). Further, at higher concentration of Mn^{2+}, it appeared that there was no substrate inhibition observed for dopamine. We can therefore use our model to propose how this takes place if substrate inhibition no longer occurs in the presence of Mn^{2+}. This would imply that the second dopamine molecule would be displaced by Mn^{2+} binding. We investigated the region of Asp-86 and found that the amine of second dopamine molecule interacts with Glu-89, which is only 4–6 Å from Asp-86 (Fig. 2*c*). Glu-89 represents the only non-hydrophobic interaction for the second dopamine molecule. We therefore propose that Mn^{2+} binding at the SULT1A3 binding site may involve both Asp-86 and Glu-89 side chains. This interaction would prevent binding of the second dopamine molecule by removing a major protein interaction. This is further supported by the fact that Glu-89 is replaced by isoleucine in SULT1A1, this protein shows very low substrate binding affinity for dopamine, and its activity is unaffected by adding Mn^{2+} (44, 45).

The mutation of Glu-89 in SULT1A3 to isoleucine results in reduced activity toward dopamine (42, 45). In the SULT1A3 crystal structure (15), residues 86–90 form a mobile loop that intercalates into the active site of a symmetry-related monomer. The residues in this region are poorly ordered and were suggested to have the potential to undergo disorder-order transition upon substrate binding. In our model of SULT1A3, this flexible loop tucks back in to the same subunit to close over the active site, as in the crystal structure of SULT1A1, and Glu-89 is placed within hydrogen-bond distance to the second dopamine molecule. Even though the mechanism for low activity remains unclear, this mutant may have altered structural interactions of the flexible loop with the substrate. Then again, the decreased overall charge of the substrate-binding pocket may make it less able to bind dopamine.

The data from these investigations support the reliability of our SULT1A3 model, as well as the previously proposed hypothesis that inhibition in SULT1A1 and SULT1A3 is caused by binding of a second substrate molecule at the substrate binding site, and suggest a major role for residue 247 in substrate inhibition of human SULT1A1.

REFERENCES

1. Falany, C. N. (1997) *FASEB J.* **11,** 1–2
2. Weinshilboum, R. M., Otterness, D. M., Aksoy, I. A., Wood, T. C., Her, C., and. Raftogianis, R. B. (1997) *FASEB J.* **11,** 3–14
3. Glatt, H. (2000) *Chem. Biol. Interact.* **129,** 141–170
4. Chou, H. C., Lang, N. P., and Kadlubar, F. F. (1995) *Cancer Res.* **55,** 525–529
5. Yamazoe, Y., Nagata, K., Yoshinari, K., Fujita, K., Shiraga, T., and Iwasaki, K. (1999) *Cancer Lett.* **143,** 103–107
6. Banoglu, E. (2000) *Curr. Drug Metab.* **1,** 1–30
7. Wang, Y., Spitz, M. R., Tsou, A. M., Zhang, K., Makan, N., and Wu, X. (2002) *Lung Cancer* **35,** 137–142
8. Seth, P., Lunetta, K. L., Bell, D. W., Gray, H., Nasser, S. M., Rhei, E., Kaelin, C. M., Iglehart, D. J., Marks, J. R., Garber, J. E., Haber, D. A., and Polyak, K. (2000) *Cancer Res.* **60,** 6859–6863
9. Zheng, W., Xie, D., Cerhan, J. R., Sellers, T. A., Wen, W., and Folsom, A. R. (2001) *Cancer Epidemiol. Biomarkers Prev.* **10,** 89–94
10. Nowell, S., Sweeney, C., Winters, M., Stone, A., Lang, N. P., Hutchins, L. F., Kadlubar, F. F., and Ambrosone, C. B. (2002) *J. Natl. Cancer Inst.* **94,** 1635–1640
11. Rikke, B. A., and Roy, A. K. (1996) *Biochim. Biophys. Acta* **1307,** 331–338
12. Nagata, K., and Yamazoe, Y. (2000) *Annu. Rev. Pharmacol. Toxicol.* **40,**

59–176
13. Blanchard, R., Freimuth, R. R., Buck, J., and Weinshilboum, R. M., and Coughtrie, M. W. H. (2004) *Pharmacogenetics* **14,** 199–211
14. Kakuta, Y., Pedersen, L. G., Carter, C. W., Negishi, M and Pedersen, L. C. (1997) *Nat. Struct. Biol.* **4,** 904–908
15. Bidwell, L. M., McManus, M. E., Gaedigk, A., Kakuta, Y., Negishi, M., Pedersen, L., and Martin. J. L. (1999) *J. Mol. Biol.* **293,** 521–530
16. Dajani, R., Cleasby, A., Neu, M., Wonacott, A. J., Jhoti, H., Hood, A. M., Modi, S., Hersey, A., Taskinen, J., Cooke, J. M., Manchee, G. R., and Coughtrie, M. W. (1999) *J. Biol. Chem.* **274,** 37862–37868
17. Kakuta, Y., Sueyoshi, T., Negishi, M., and Pedersen, L. C. (1999) *J. Biol. Chem.* **274,** 10673–10676
18. Pedersen, L. C., Petrotchenko, E. V., and Negishi, M. (2000) *FEBS Lett.* **475,** 61–64
19. Rehse, P. H., Zhou, M., and Lin, S. X. (2002) *Biochem. J.* **364,** 165–171
20. Pedersen, L. C., Petrotchenko, E., Shevtsov, S., and Negishi, M. (2002) *J. Biol. Chem.* **277,** 17928–17932
21. Gamage, N. U., Duggleby, R. G., Barnett, A. C., Tresillian, M., Latham, C. F., Liyou, N. E., McManus, M. E., and Martin, J. L. (2003) *J. Biol. Chem.* **278,** 7655–7662
22. Ganguly, T. C., Krasnykh, V., and Falany, C. N. (1995) *Drug Metab. Dispos.* **23,** 945–950
23. Reiter, C., Mwaluko, G., Dunnette, J., Van Loon, J., and Weinshilboum, R. (1983) *Naunyn-Schmiedeberg's Arch. Pharmacol.* **324,** 140–147
24. Raftogianis, R. B., Wood, T. C., and Weinshilboum, R. M. (1999) *Biochem. Pharmacol.* **58,** 605–616
25. Gaedigk, A., Beatty, B. G., and Grant, D. M. (1997) *Genomics* **40,** 242–246
26. Brix, L. A., Duggleby, R. G., Gaedigk, A., and McManus, M. E. (1999) *Biochem. J.* **337,** 337–343
27. Foldes, A., and Meek, J. L. (1973) *Biochim. Biophys. Acta* **327,** 365–374
28. Jones, G., Willett, P., Glen, R. C., Leach, A. R., and Taylor, R. (1997) *J. Mol. Biol.* **267,** 727–748
29. Brunger, A. T., Adams, P. D., Clore, G. M., DeLano, W. L., Gros, P., Grosse-Kunstleve, R. W., Jiang, J. S., Kuszewski, J., Nilges, M., Pannu, N. S., Read, R. J., Rice, L. M., Simonson, T., and Warren, G. L. (1998) *Acta Crystallogr. Sect. D Biol. Crystallogr.* **54,** 905–921
30. Laskowski, R. A., Macarthur, M. W., Moss, D. S., and Thornton, J. M. (1993) *J. Appl. Crystallogr.* **26,** 283–391
31. Zhang, H., Varmalova, O., Falany, F. M., and Lehy, T. S. (1998) *J. Biol. Chem.* **273,** 10888–10892
32. Yoshinari, K., Petrotchenko, E. V., Pedersen, L. C., and Negishi, M. (2001) *J. Biochem. Mol. Toxicol.* **15,** 67–75
33. Lewis, A. J., Kelly, M. M., Walle, U. K., Eaton, E. A., Falany, C. N., and Walle, T. (1996) *Drug Metab. Dispos.* **24,** 1180–1185
34. Kester, M. H. A., Kaptein, E., Roest, T. J., van Dijk, C., Tibboel, D., Meinl, W., Glatt, H., Coughtrie, M. W. H., and Visser, T. J. (1999) *J. Clin. Endocrinol. Metab.* **84,** 1357–1369
35. Harris, R. M., Waring, R. H., Kirk, C. J., and Hughes, P. J. (2000) *J. Biol. Chem.* **275,** 159–166
36. Honma, W., Kamiyama, Y., Yoshinari, K., Sasano, H., Shimada, M., Nagata, K., and Yamazoe, Y. (2001) *Drug. Metab. Dispos.* **29,** 274–281
37. Li, X., Clemens, D. L., Cole, J. R., and Anderson, R. J. (2001) *J. Endocrinol.* **171,** 525–532
38. Chen, G., Rabjohn, P. A., York, J. L., Wooldridge, C., Zhang, D., Falany, C. N., and Rodominska-Pandya, A. (2000) *Biochemistry* **39,** 16000–16007
39. Chen, G., and Chen, X. (2003) *J. Biol. Chem.* **278,** 36358–36364
40. Dajani, R., Hood, A. M., and Coughtrie, M. W. (1998) *Mol. Pharmacol.* **54,** 942–948
41. Brix, L. A., Barnett, A. C., Duggleby, R. G., Leggett, B., and McManus, M. E. (1999b) *Biochemistry* **38,** 10474–10479
42. Liu, M. C., Suiko, M., and Sakakibara, Y. (2000) *J. Biol. Chem.* **275,** 13460–13464
43. Sakakibara, Y., Takami, Y., Nakayama, T., Suiko, M., and Liu., M. C. (1998) *J. Biol. Chem.* **273,** 6242–6247
44. Pai, T. G., Ohkimoto, K., Sakakibara, Y., Suiko, M., Sugahara, T., and Liu, M. C. (2002) *J. Biol. Chem.* **277,** 43813–43820
45. Pai, T. G., Oxendine, I., Sugahara, T., Suiko, M., Sakakibara Y., and Liu, M. C. (2003) *J. Biol. Chem.* **278,** 1525–1532